

SHAPE AND SIZE RELATIONSHIP OF SEVERAL LUNAR DUSTS: PRELIMINARY RESULTS.

Lawrence A. Taylor¹, Yang Liu¹, and Aicheng Zhang^{1,2}. ¹Planetary Geosciences Institute, Dept. of Earth & Planetary Sciences, Univ. of Tennessee, Knoxville, TN 37996. (lataylor@utk.edu); ² Purple Mountain Observatory, Nanjing 21008, China.

Introduction: Before establishing a human outpost on the Moon, numerous problems associated with lunar dust must be addressed and mitigated [1, 2]. The deleterious nature of lunar dusts was experienced during all Apollo missions. Lunar dusts (brought in on dirty spacesuits and boots) contaminated the atmosphere in the lunar module and irritated the eyes, sinuses, and throats of the astronauts [1, 2]. In contrast to short exposure times during the Apollo missions, astronauts partaking in missions of extended presence on the Moon will be subjected to prolonged exposure, if lunar dust contamination is not substantially mitigated. The physiology effects of lunar dusts on humans are being actively studied by a multi-discipline group of scientists, *Lunar Airborne Dust Toxicity Analyses Group* (LADTAG) (e.g. [3-5]). Lunar dust, $< 20 \mu\text{m}$ fraction of the lunar soil (definition adopted by LADTAG), consists of ~ 20 wt% of lunar soil [6,7]. Detailed information of the lunar dust properties, chemistry and mineralogy, particle size distribution (PSD), particle shape, magnetic susceptibility, and electrostatic properties, is important for quantitative interpretation of such studies. To achieve this, our group has conducted analyses on chemistry and mineralogy [8, 9], size distribution [10, 11], shape characterization [12] of different lunar soil ($< 1 \text{ mm}$ regolith) and dust ($< 20 \mu\text{m}$ soil) samples. We also developed a technique to separate $< 3 \mu\text{m}$ fraction of lunar soils from the bulk sample [13,14].

Previous Results: PSD results show lunar dusts have a large number of particles at 0.1 or $0.3 \mu\text{m}$, much smaller than the lunar soil simulant (Fig. 1). The fine grain size of lunar dust points to the importance of detailed characterization of particle shapes. Particle types (glass beads, vesicular, etc.) and their relationship with particle size were broadly discussed but not quantitatively assessed in [11]. In order to quantify the distribution of shape with size, two shape factors were used in Liu et al. [11]: aspect ratio and complexity factor. The former is an indicator of elongation. For our definition, the smaller the number is, the more elongated it becomes. Complexity factor measures the irregularity of the particle shape. The distribution of shape was categorized into two fractions ($< 1 \mu\text{m}$ and $> 1 \mu\text{m}$) and no significant difference was found between the two groups. Because all $> 1 \mu\text{m}$ grains were grouped together, the relationship between shape and size cannot be determined. As an extension of our

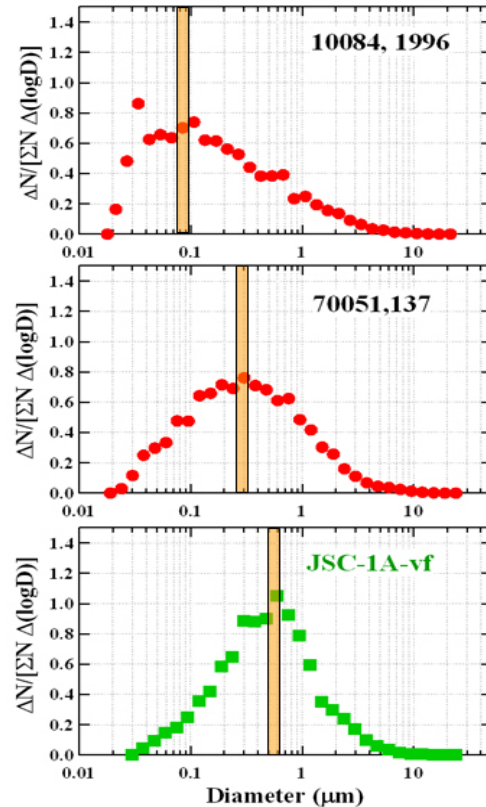


Figure 1. Particle size distribution of the $< 45 \mu\text{m}$ fraction of two lunar soils and a lunar soil simulant [10].

study [11], we examine if there is any systematic change of particle shapes and types with particle size at $> 1 \mu\text{m}$ size. Here we report preliminary results.

Additional Data Processing: Data used in this study are the same as in Liu et al. [11] and Park et al. [10], where thousands of particles were measured and characterized for each sample. Shape parameters (aspect ratio and complexity factor) were defined as in [11]. For $> 1 \mu\text{m}$ particles, distribution of shape factors was obtained for three arbitrarily-defined size fractions: $1\text{-}3 \mu\text{m}$, $3\text{-}5 \mu\text{m}$, and $> 5 \mu\text{m}$. Point counting technique was implemented for studying particle types. For simplicity, particle type was categorized into: vesicular, spherical, and others.

Results and Discussion: Preliminary results from point counting of particle types suggest that vesicular grains and sphere decrease in abundances with grain size. As small lunar soil particulates are generally

broken from larger ones, the decreasing abundances of vesicular grains are expected. Spherical grains are glass beads produced mostly by micro-meteorite impacts, but also by fire-fountain pyroclastic activity forming volcanic glass beads, such as the orange soil at Apollo 17 Shorty Crater (74220) collected by astronaut Harrison H. (Jack) Schmitt. The population of the vesicular (swiss-cheese texture) and spherical grains decrease rapidly in the less than 1 μm fraction, and is virtually absent by 500-566 nm.

Shape distributions of two lunar samples in three size fractions are shown in Figures 1 and 2. Apollo 12 12001 and Apollo 17 79221 are the less mature and more mature samples in our studies, respectively. Maturity is proportional to the amount of nanophase metallic iron (see [15, 16] for definition of maturity). The $>1 \mu\text{m}$ fraction was reported in [12], represents the average distribution of the three size fractions.

Aspect Ratio: Different size fractions show subtle difference in the peak positions of the distribution curves: increasing slightly with decreasing grain size. This change indicates that particles become increasingly rounded at smaller sizes. However, the 1-3 μm fraction shows the most diverse in elongation (a small but significant numbers at a.r. <0.3 . Because the 1-3 μm fraction is the most abundant size of all particles measured, it dominants the average distribution curve.

Complexity factor: There is a subtle decrease in complexity with decreasing size (by ~ 0.05). Particles $> 5 \mu\text{m}$ tend to have more complex shapes (more jagged/irregular) with a significant number at >1.5 .

Summary: Our preliminary data show increasing smoothness and elongation with decreasing size, an interesting result deserves further study. These data provide basis for quantitative experimentation into understanding the toxicity effects of lunar soil.

References: [1] Gaier J. R. (2005) NASA, GRC. NASA/TM-2005-213610. [2] Taylor L. A. et al. (2005) *1st Space Explor. Conf., AIAA*. [3] Lam C.-W. et al. (2008) *NLSI Lunar Science Conf.*, Abstract # 2136. [4] Khan-Mayberry N.N. (2008) *NLSI Lunar Science Conf.*, Abstract # 2081. [5] Jones L. et al. (2008). *NLSI Lunar Science Conf.*, Abstract # 2100. [6] Carrier, W.D. III (2003). *J. Geotech. Geoenvir. Eng.*, 129, ASCE, 956-959. [7] McKay, D. S. et al. (1991). *Lunar Sourcebook*, Cambridge University Press, New York, 286-356. [8] Taylor L. A. et al. (2001) *JGR*, 106, 27985-27999. [9] Taylor L. A. et al. (2003) *LPS XXXIV*, Abstract # 1774. [10] Park J. S. et al. (2008) *JAE*, 21, 266-271. [11] Liu Y. et al. (2008) *NLSI conf.*, Abstract 2072. [12] Liu Y. et al. (2008) *JAE*, 21, 272-279. [13] Schnare D. W. et al. (2008) *LPS XXXIX*, Abstract #1156. [14] Liu Y. et al. (2008) *PSS*, 56, 1517-1523. [15] Morris R. V. (1976) *LPSC VII*, 315-335. [16] Morris R. V. (1978) *LPSC IX*, 2287-2297.

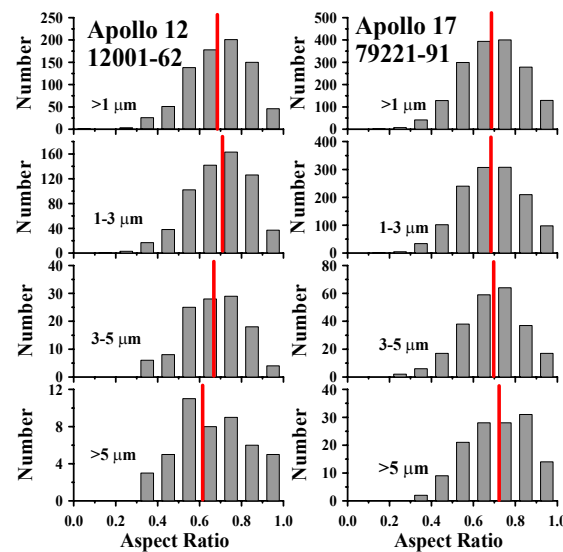


Figure 2. Distribution aspect ratio of Apollo 12, 12001 and Apollo 17, 79221 dusts in different size fractions. Numbers after sample name is the maturity index. The $>1 \mu\text{m}$ distribution curve shows the average of three size fractions. Red lines mark the peak positions for each curve.

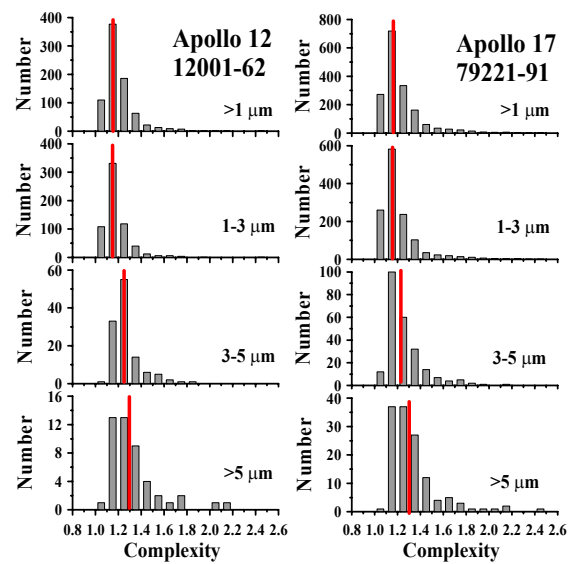


Figure 3. Distribution aspect ratio of Apollo 12, 12001 and Apollo 17, 79221 dusts in different size fractions. Numbers after sample name is the maturity index. The $>1 \mu\text{m}$ distribution curve shows the average of three size fractions. Red lines mark the peak positions of each curve.